

Short communication

Enhanced cycle performance of Li–S battery with a polypyrrole functional interlayer



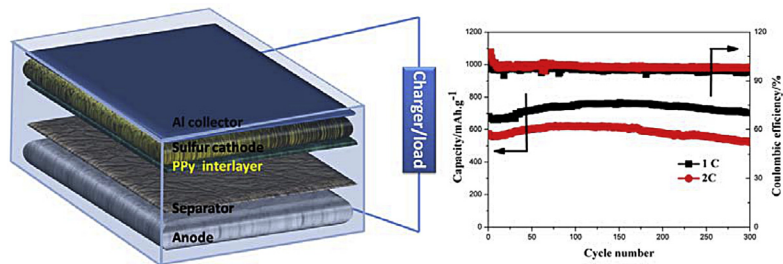
Guoqiang Ma, Zhaoyin Wen*, Jun Jin, Meifen Wu, Xiangwei Wu, Jingchao Zhang

CAS Key Laboratory of Materials for Energy Conversion, Shanghai Institute of Ceramics, Chinese Academy of Sciences, Shanghai 200050, PR China

HIGHLIGHTS

- Polypyrrole functional interlayer (PFIL) was in-situ fabricated uniformly onto the surface of sulfur cathode.
- Polypyrrole functional interlayer improve the cycling performance of Li–S batteries significantly.
- This work is focused on the structural design of novel interlayer for Li–S batteries.

GRAPHICAL ABSTRACT



ARTICLE INFO

Article history:

Received 31 January 2014

Received in revised form

27 April 2014

Accepted 7 May 2014

Available online 21 May 2014

Keywords:

Lithium sulfur battery

Sulfur cathode

Functional interlayer

Conductive polymer

Cycle performance

ABSTRACT

Polypyrrole functional interlayer is in-situ fabricated uniformly onto the surface of sulfur cathode to inhibit the dissolution of lithium polysulfides and protect sulfur cathode. Li–S battery with the functional interlayer shows an encouraging electrochemical performance. The initial discharge capacity is 719 mAh g^{-1} and the capacity retains at 846 mAh g^{-1} even after 200 cycles at 0.2C with an average coulombic efficiency of 94.2%. Moreover, the discharge capacities are 703 mAh g^{-1} and 533 mAh g^{-1} at 1C and 2C respectively even after 300 cycles.

© 2014 Elsevier B.V. All rights reserved.

1. Introduction

Currently, with the rapid development of zero-emission electric vehicles (EV) and smart grids, rechargeable batteries with high energy density and long cycle life are in great demand [1,2]. Among various battery systems, lithium sulfur (Li–S battery) has a high theoretical capacity (1675 mAh g^{-1}) and a high theoretical specific

energy (2600 Wh Kg^{-1}). In combination with the natural abundance, low cost and environmental friendliness of sulfur, Li–S battery becomes a promising candidate for the next generation portable energy sources [3,4]. However, the insulating nature of sulfur, the volume expansion, and the high solubility of lithium polysulfides (PS) in the liquid electrolyte lead to high polarization, serious capacity fading, poor rate stability and low coulombic efficiency of Li–S battery, inhibiting its commercialization [3,4]. Many approaches have been proposed to address these obstacles and improve the electrochemical performance of Li–S battery. Most studies are focusing on embedding sulfur in/on various forms of carbon, such as graphene [5,6], carbon nanotubes [7,8], carbon spheres [9,10], micro/mesoporous carbons [11], etc, which can

* Corresponding author. Shanghai Institute of Ceramics, Chinese Academy of Sciences, 1295 DingXi Road, Shanghai 200050, PR China. Tel.: +86 21 52411704; fax: +86 21 52413903.

E-mail addresses: zywen@mail.sic.ac.cn, gxzhang@student.sic.ac.cn (Z. Wen).

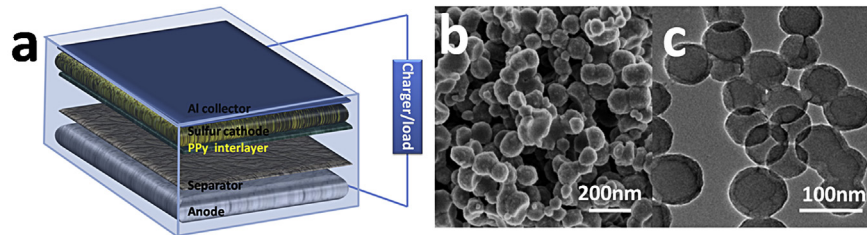


Fig. 1. The schematic of the functional interlayer in the lithium sulfur battery (a), SEM (b) and TEM (c) images of PPy nano-particles.

improve the conductivity of the cathode. Furthermore, surface coating of sulfur with conductive polymers [12,13] and oxides [14] are effective approaches to suppress the dissolution and migration of lithium polysulfides, resulting in enhanced cycle performance. The modification of the electrolyte [15,16] and the protection of lithium anode [17] are also effective strategies to improve the electrochemical performance of Li–S batteries. However, the obtained success from the modification of electrolyte and anode is limited. Although studies on the cathode show promising improvements, but the material processing steps are often complex and expensive, limiting the feasibility of manufacturing a viable Li–S battery [3]. Therefore, more effective approaches are necessary to be set up for the commercialization of Li–S battery.

Recently, microporous carbon paper [18], free standing MWCNT paper [19], reduced graphene oxide based films [20] and treated carbon paper [21] have been added between sulfur cathode and separator as the carbon interlayer. The carbon interlayer facilitates the adsorption of soluble lithium polysulfides and makes them available for reutilization during the following cycles. Moreover, the carbon interlayer can reduce the polarization of the cell significantly. The cycle performance is enhanced self-evidently with the simple strategy. However, the long-term cycle performance still needs to be improved owing to the weak adsorbing ability of carbon to lithium polysulfides. Moreover, the large weight of interlayer reduces the energy density of the battery.

It is reported that conductive polymers such as polyaniline (PAN), polypyrrole (PPy), and polythiophene (PTh) usually are proton-doped so that they can act as bridges to link the polymer to PS anions via H-bonds [3,22]. The H-bonds between the proton-doped polymers and lithium polysulfides make them adsorb PS more effective during charge/discharge process [22]. Meanwhile, the conductive polymers are both electronically conductive and ionically conductive, which are beneficial to reduce the resistance and enhance the rate capability of the cell [23]. Furthermore, the conductive polymers themselves are electrochemically active, which can provide some capacity for the cell. Thus conductive polymers are more suitable to be used as the functional interlayer for Li–S battery.

CMK-8 is a kind of 3-dimensional highly conductive mesoporous carbon, which has been widely used in supercapacitors and catalytic. In our previous report, the mesoporous carbon CMK-8 was prepared and acted as the matrix to load sulfur for the first time, an attractive cycle performance was obtained [24]. Herein, as seen in Fig. 1a, PPy functional interlayer (PFIL) is in-situ fabricated on the surface of CMK-8/S cathode to further enhance the cycle performance. SEM and TEM images of PPy-nanoparticles fabricated with the same method are shown in Fig. 1b and c, PPy nano-particles are around 80 nm. Because of the H-bond and large specific area, PFIL composed of PPy nano-particles can inhibit the dissolution and migration of PS in the electrolyte effectively. And PFIL can also protect the structure of sulfur cathode from being damaged during charge/discharge process. Moreover, the mass of the PFIL is much smaller than that of the other interlayer mentioned above. So the

novel configuration presented here is more suitable to be applied to overcome the problems of Li–S battery.

2. Experimental

2.1. Preparation of the sulfur cathode

The CMK-8/S composite (65% S content) was prepared as described earlier [24]. To prepare a cathode, the slurry was prepared by ball milling 80% CMK-8/S composite, 10 wt% acetylene black (AB) (>99.5%, Sinopharm Chemical Reagent Co.) as conductive agent, 10 wt% polyvinylidenefluoride (PVDF) (>99%, Shanghai Oflourine Chemical Technology Co) as the binder and *N*-methyl-2-pyrrolidone (NMP) (>99.5%, Sinopharm Chemical Reagent Co.) as the solvent. The slurry was casted onto aluminum foil substrates. After the solvent evaporated, the cathode of Li–S battery was obtained. The mass of sulfur in the cathode was around 1.5 mg cm⁻².

2.2. Addition of the functional interlayer

The PFIL was fabricated as follows: firstly, 0.2 mol Py and 0.5 mol CH₃COOH were dispersed into 90 ml deionized water and 10 ml alcohol, denoted as solution A, and 0.2 mol (NH₄)₂S₂O₈ was dissolved in 100 ml deionized water, denoted as solution B. Secondly, the sulfur cathode prepared above was soaked into solution A for 10 s, then it was soaked into solution B for 10 s, then it was soaked into deionized water to remove the excess (NH₄)₂S₂O₈. Thirdly, the second step was repeated for 3 times to obtain sufficiently thick PPy functional interlayer (PFIL) on the surface of sulfur cathode. The thickness of PFIL was around 10 μm, and the mass of PFIL was around 0.3 mg cm⁻². The PPy nano-particles were fabricated separately as follow, the solution was added dropwise into solution B and stirred for 12 h at room temperature. The product was washed and filtered until the filtrate was colorless. Finally, the products were dried under vacuum at 60 °C for 12 h.

2.3. Preparation of coin-type cell

The cathode was dried at 60 °C under vacuum for 24 h and then cut into circles with 14 mm in diameter. CR2025 type coin cells were assembled in a glove box with oxygen and water contents less than 1 ppm. A solution of 1 M LiTFSI dissolved in DOL/DME/PyR₁₄TFSI (v/v/v, 2/2/1) was employed as the electrolyte. The cells contained GF/A film as the separator and lithium foils as both the counters and reference electrodes.

2.4. Characterization

The cells after 50 cycles were disassembled in an argon-filled glove-box. Then the Li anode and sulfur cathodes were further enclosed in a sealed vessel which was filled with Ar gas for further testing. SEM images were measured by field emission scanning electron microscope (FESEM JSM-6700) and scanning electron

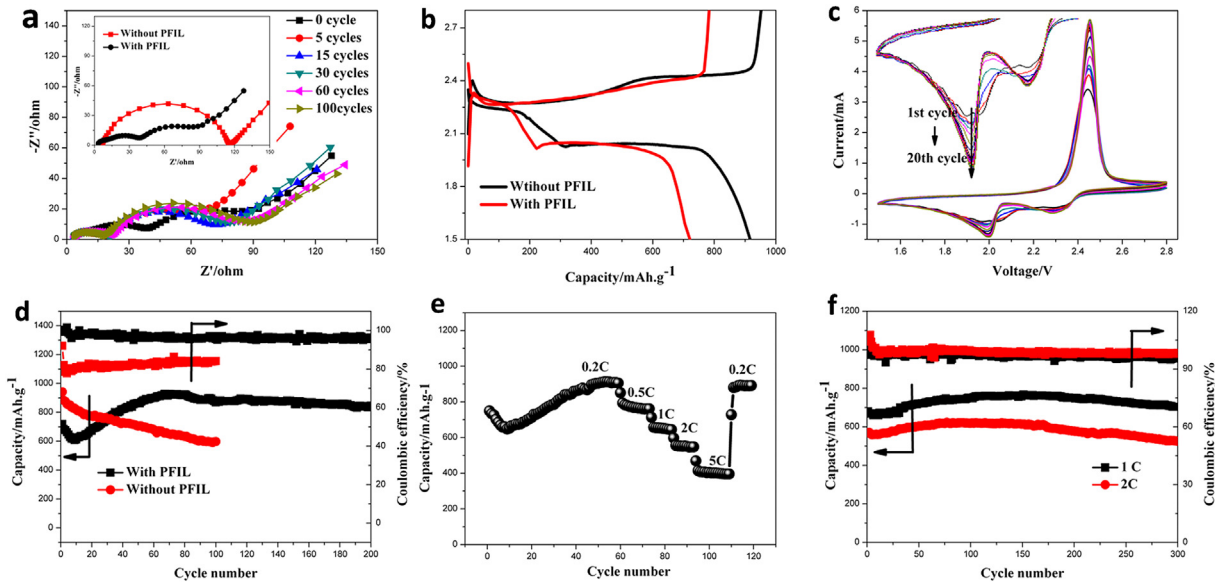


Fig. 2. (a) Electrochemical impedance spectroscopy plots of Li–S battery with PFIL in different cycles after fully charged to 2.8 V at 0.2C, the inset in (a) is electrochemical impedance spectroscopy plots of Li–S batteries with and without PFIL, (b) the charge/discharge curves of the Li–S battery with and without PFIL, (c) the CV profiles of the Li–S battery with PFIL, (d) the cycle performance and coulombic efficiencies of Li–S battery with and without PPy layer at 0.2C, (e) the rate performance of the Li–S battery with PFIL, (f) cycle performance of Li–S batteries with PFIL at 1C and 2C for prolonged cycles.

microscope (Hitachi S-3400N). Transmission electron microscopy (TEM) images were measured on a JEOL JEM-2010 transmission electron microscope. AC impedance measurement was carried out by a Frequency Response Analyzer (FRA) technique on an Autolab Electrochemical Workstation over the frequency range from 0.1 Hz to 10 MHz with the amplitude of 10 mV. Cyclic-voltammetry (CV) measurement was also conducted using the Autolab Electrochemical Workstation. The galvanostatic charge and discharge tests were conducted on a LAND CT2001A battery test system in a voltage range of 1.5–2.8 V (vs. Li/Li⁺) at different current densities. The cycle performance of the battery with PFIL was obtained from more than five tested batteries.

3. Results and discussion

Electrochemical impedance spectroscopy (EIS) is used to study the electrochemical behavior of the battery. The resistance of the cell is composed of electrolyte resistance (R_e), the charge transfer resistance (R_c) and the interfacial resistance (R_i). However, as shown in Fig. 2a, there is only one semicircle in the Nyquist plots of the Li–S cell without PFIL, it seems that the R_i is so small, thus the semicircle corresponds to the charge transfer resistance (R_c) of the cell [13,25]. There is the other semicircle in the Nyquist plots of the Li–S cell with PFIL, corresponding to the resistance of the PFIL (R_p), which may be due to the reaction between functional groups and the electrolyte [21]. R_c decreases largely with the addition of PFIL, indicating a weak polarization for the Li–S battery with PPy interlayer. Because of the shuttle effect during charge/discharge process, the redistribution of active material is unavoidable for Li–S battery. This results in an inhomogeneous distribution of insulating sulfur on the surface of cathode and the corrosion of lithium anode, leading to the increased resistance during charge/discharge process [26]. As shown in Fig. 2a, the value of R_c before discharge is 41 Ω. It decreases dramatically to the lowest value (20.4 Ω) at the 5th cycle, indicating electrochemical activation process, subsequently, the resistance value maintains at around 21 Ω during 15th–100th cycles. The stable R_c suggests that the deposition and aggregation of insulating material on the surface of electrode are not serious,

indicating an outstanding cycle performance. And R_p increases slightly from 55 Ω before cycling to 76 Ω after 100 cycles, which can be attributed to the deposition of insulating sulfur on the surface of PPy nanoparticles.

The charge/discharge profiles of Li–S battery with PFIL and without PFIL (Fig. 2b) show that there are two discharge plateaus at 2.3 V and 2.1 V corresponding to the generation of PS and Li₂S₂/Li₂S respectively [27,28]. This indicates that the addition of PFIL in the Li–S battery does not change the electrochemical reactions. However, PFIL decreases the contact performance between active material and liquid electrolyte to some extent, so not all the active material is used during the first discharge process. Therefore, Li–S battery with PFIL shows a lower initial discharge specific capacity (719 mAh g⁻¹) than that of the cell without PFIL (940 mAh g⁻¹). As seen in the CV curves (Fig. 2c), the areas of reduction peaks increase during the 1–10 cycles, the anodic and cathodic peaks are almost overlapping during 10–20 cycles, suggesting a high reversibility in the following cycles.

The cycle performance of the Li–S cell with PFIL at 0.2C is displayed in Fig. 2d. With an apparent capacity fading during the first several cycles, the specific capacity increases slowly during 10–80 cycles, which is consistent with the CV curves. Afterward, the discharge specific capacity sustains at as high as 846 mAh g⁻¹ even after 200 cycles with an average coulombic efficiency of 94.2%. While the capacity of Li–S battery without PFIL is only 587 mAh g⁻¹ after 100 cycles with the average coulombic efficiency of 83.4%. The apparent capacity fading during the first several cycles is attributed to shuttle effect. Meanwhile, the dissolved PS during charge/discharge process is absorbed by PPy nano-particles other than migrate to lithium anode, which is reutilized at the following cycles. In addition with a better contact between electrolyte and active material after cycling, the utilization rate of the active material is hence increased, which is consistent with the results of CV curves and the increased discharge capacity during 10–80 cycles. Moreover, the adsorption effect between PPy and lithium polysulfides suppresses the shuttle effect during charge/discharge process. So the Li–S battery with PFIL owes an excellent cycle performance and high coulombic efficiencies. Moreover, the cycle

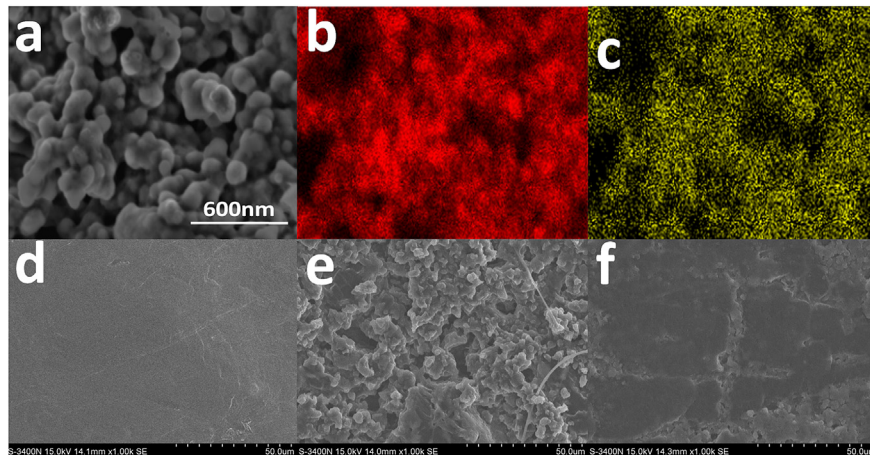


Fig. 3. (a) SEM image of the surface of the PFIL after 50 cycles, the element C (b) and S(c) mapping of the same area in (a), SEM image of fresh Li anode (d), Li anode without PFIL after 50 cycles (e), and Li anode with PFIL after 50 cycles (f). All the images are obtained from the batteries after fully charged.

performance of the other batteries with PFIL is also shown in Fig. S1, they all show a similar trend, indicating that the experimental results can be repeated.

As seen in Fig. 2e, the cell with the PFIL delivers a reversible capacity of 415 mAh g^{-1} at 5C. Moreover, the discharge capacity returns to 901 mAh g^{-1} when the rate decreases from 5C to 0.2C. In addition, the Li–S battery with PFIL displays good rate stability with discharge capacities of 703 mAh g^{-1} and 533 mAh g^{-1} at 1C and 2C respectively even after 300 cycles. The coulombic efficiencies reach above 96% at the whole cycles. The excellent cycle performance and rate stability should be related to the stable structure and good conductivity of the sulfur cathode [29]. Firstly, the cubic mesoporous carbon (CMK-8) is used as the matrix of sulfur, supplying a 3D conductive networks for sulfur. The dual conductive PFIL is fabricated on the surface of cathode, which indicates a fast electronic and Li^+ kinetics. Secondly, the H-bond and large specific area of PPy nano-particles supply a strong adsorption effect between PPy and PS. The dissolution and migration of PS in the electrolyte is inhibited effectively, so the capacity fading owing to shuttle effect is suppressed. Moreover, the structural damage of the cathode coming from the volume expansion is buffered because of the addition of the flexible PFIL on the surface.

To determine the adsorption effect of PPy to PS and S, the surface morphology of the PFIL after 50 cycles is observed in Fig. 3a. PPy nano-particles adhere to each other, and the diameter of nano-particles is around 120 nm, which is bigger than that of PPy nano-particles fabricated before using the same method (as shown in Fig. 1b and c). C and S elements have the same distribution as the PPy nano-particles, suggesting that there is elemental sulfur coating onto the surface of PPy nano-particles. It was reported that not all the Li_2S was oxidized to sulfur, so the material coated on the surface of PPy nano-particles consist of sulfur and PS [30]. It is observed in Fig. 3e that the lithium anode without PFIL after cycling is loosely packed, suggesting serious corrosion of lithium anode [16]. However, the surface of lithium anode becomes uniform with PFIL addition (Fig. 3f), demonstrating that the addition of PFIL evidently inhibit the dissolution and migration of PS in the electrolyte, thus the corrosion reaction between lithium anode and PS is suppressed effectively.

4. Conclusion

In summary, a functional interlayer composed of PPy nano-particles is in-situ fabricated on the surface of sulfur cathode using a simple method to substantially improve the electrochemical

performance of Li–S battery. PFIL can not only inhibit the redistribution of sulfur during charge/discharge process and reduce the polarization of the cell, but also suppress the shuttle effect during charge/discharge process owing to the adsorption effect of PPy nano-particles to PS. Simultaneously, the volume expansion of the sulfur cathode is buffered to some extent by PFIL composed of PPy nano-particles. The strategy proposed in this study could be helpful to explore and develop new functional interlayer between anode and cathode of Li–S battery, such as the other conductive polymer, Li^+ conductor ceramic particles and so on.

Acknowledgments

This work was financially supported by NSFC Project No. 51373195 No. 51372262 and No. 51272267; research projects from the Science and Technology Commission of Shanghai Municipality No. 08DZ2210900.

We thank Prof. B. V. R. Chowdari (Department of Physics, National University of Singapore) for helpful discussions.

Appendix A. Supplementary data

Supplementary data related to this article can be found at <http://dx.doi.org/10.1016/j.jpowsour.2014.05.057>.

References

- [1] S.A. Freunberger, Peter G. Bruce, Laurence J. Hardwick, Jean-Marie Tarascon, *Nat. Mater.* 11 (2012) 19–29.
- [2] Z.Y. Wen, J.Z. Li, *J. Inorg. Mater.* 28 (2013) 1163–1164.
- [3] S.S. Zhang, *J. Power Sources* 231 (2013) 153–162.
- [4] Y. Yang, G. Zheng, Y. Cui, *Chem. Soc. Rev.* 42 (2013) 3018–3032.
- [5] C. Zu, A. Manthiram, *Adv. Energy Mater.* 3 (2013) 1008–1012.
- [6] L. Yin, J. Wang, F. Lin, J. Yang, Y. Nuli, *Energy Environ. Sci.* 5 (2012) 6966–6972.
- [7] M. Hagen, S. Dorfler, H. Althues, J. Tubke, M.J. Hoffmann, S. Kaskel, K. Pinkwart, *J. Power Sources* 213 (2012) 239–248.
- [8] C. Jia-jia, J. Xin, S. Qiu-jie, W. Chong, Z. Qian, Z. Ming-sen, D. Quan-feng, *Electrochim. Acta* 55 (2010) 8062–8066.
- [9] G. He, S. Evers, X. Liang, M. Cuisinier, A. Garsuch, L.F. Nazar, *ACS Nano* 7 (2013) 10920–10930.
- [10] N. Jayaprakash, J. Shen, S.S. Moganty, A. Corona, L.A. Archer, *Angew. Chem. Int. Ed.* 50 (2011) 5904–5908.
- [11] S. Xin, L. Gu, N.H. Zhao, Y.X. Yin, L.J. Zhou, Y.G. Guo, L.J. Wan, *J. Am. Chem. Soc.* 134 (2012) 18510–18513.
- [12] Y. Yang, G.H. Yu, J.J. Cha, H. Wu, M. Vosgueritchian, Y. Yao, Z.A. Bao, Y. Cui, *ACS Nano* 5 (2011) 9187–9193.
- [13] G.C. Li, G.-R. Li, S.-H. Ye, X.-P. Gao, *Adv. Energy Mater.* 2 (2012) 1238–1245.
- [14] Z.W. Seh, W. Li, J.J. Cha, G. Zheng, Y. Yang, M.T. McDowell, P.C. Hsu, Y. Cui, *Nat. Commun.* 4 (2013) 1331–1336.

- [15] K. Jeddi, K. Sarikhani, N.T. Qazvini, P. Chen, J. Power Sources 245 (2014) 656–662.
- [16] G.Q. Ma, Z.Y. Wen, J. Jin, M.F. Wu, G.X. Zhang, X.W. Wu, J.C. Zhang, Solid State Ionics (2014), <http://dx.doi.org/10.1016/j.ssi.2013.10.012>.
- [17] Y.M. Lee, N.-S. Choi, J.H. Park, J.K. Park, J. Power Sources 119–121 (2003) 964–972.
- [18] B. Zhang, X. Qin, G.R. Li, X.P. Gao, Energy Environ. Sci. 3 (2010) 1531–1537.
- [19] Y.S. Su, A. Manthiram, Chem. Commun. 48 (2012) 8817–8819.
- [20] X. Wang, Z. Wang, L. Chen, J. Power Sources 242 (2013) 65–69.
- [21] C. Zu, Y.S. Su, Y. Fu, A. Manthiram, Phys. Chem. Chem. Phys. 15 (2013) 2291–2297.
- [22] W. Li, Q. Zhang, G. Zheng, Z.W. Seh, H. Yao, Y. Cui, Nano Lett. 13 (2013) 5534–5540.
- [23] Y.M. Cui, Z. Wen, X. Liang, Y. Lu, J. Jin, M. Wu, X. Wu, Energy Environ. Sci. 5 (2012) 7893–7897.
- [24] G.Q. Ma, Z.Y. Wen, J. Jin, Y. Lu, K. Rui, X.W. Wu, M.F. Wu, J. Zhang, J. Power Sources 254 (2014) 353–359.
- [25] N.A. Canas, K. Hirose, B. Pascucci, N. Wagner, K.A. Friedrich, R. Hiesgen, Electrochim. Acta 97 (2013) 42–51.
- [26] J. Zheng, M. Gu, C. Wang, P. Zuo, P.K. Koech, J.G. Zhang, J. Liu, J. Xiao, J. Electrochem. Soc. 160 (2013) A1992–A1996.
- [27] N.A. Canas, S. Wolf, N. Wagner, K.A. Friedrich, J. Power Sources 226 (2013) 313–319.
- [28] X. Liang, Z.Y. Wen, Y. Liu, H. Zhang, J. Jin, M.F. Wu, X.W. Wu, J. Power Sources 206 (2012) 409–413.
- [29] N. Li, M. Zheng, H. Lu, Z. Hu, C. Shen, X. Chang, G. Ji, J. Cao, Y. Shi, Chem. Commun. 48 (2012) 4106–4108.
- [30] Y. Diao, K. Xie, S. Xiong, X. Hong, J. Electrochem. Soc. 159 (4) (2012) A421–A425.